Journal of Mines, Metals and Fuels, *73(4): 1077-1087; 2025. DOI: 10.18311/jmmf/2025/48326*

Print ISSN : 0022-2755

Journal of Mines, Metals and Fuels

Contents available at: *www.informaticsjournals.co.in/index.php/jmmf*

Comparative Evaluation of Mechanical, Chemical and Microstructural Properties of Thermo-Mechanically Treated Bars from Different Brands

Sourav Basu[1], Sourav Debnath[2]*, Pragnan Biswas[3], Soumya Mukherjee[4] and Akshay Kumar Pramanick[5]

[1,4]Department of Metallurgical Engineering, Kazi Nazrul University, Asansol - 713340, West Bengal, India
[2]Department of Electrical and Electronics Engineering, Swami Vivekananda Institute of Science and Technology, Kolkata -700145, West Bengal, India; dr.souravdebnath@gmail.com
[3]Computer and Energy Engineering, Arizona State University, Arizona - 85281, USA
[5]Department of Metallurgical and Material Engineering, Jadavpur University, Kolkata - 700032, West Bengal, India

Abstract

Thermo-Mechanically Treated (TMT) Bars are essential materials in the construction industry, valued for their high strength, ductility, and cost-effectiveness. Their properties are influenced by chemical composition and manufacturing parameters. This study evaluates the quality of two Fe-500 grade TMT bars from TATA and SAIL, both with a nominal diameter of 16 mm. The evaluation includes physical, mechanical, and chemical tests, such as microstructure analysis, hardness testing, tensile testing, and corrosion behavior under various conditions. Metallographic and optical microscopy revealed distinct microstructures, with tempered martensite on the outer ring and ferrite-pearlite in the inner core. Hardness testing was conducted using a Vickers Hardness Tester, and corrosion tests were performed in a 0.9 M NaOH solution. Tensile tests were carried out at a strain rate of 10e-3. Based on the results from these electrochemical and mechanical tests, the sample with superior properties was selected.

Major Findings: *Sample A showed superior strength characteristics, while Sample B showed greater ductility. Sample B showed higher corrosion resistance than sample A. Finally, studying the overall results, Sample B is the recommended choice over Sample A for constructing electric furnace or other electrical equipment.*

Keywords: Corrosion, Hardness, Heat Treatment, Surface Morphology, TMT Bar, Tensile Test

1.0 Introduction

Thermo-Mechanically Treated Bars (TMT Bars) are specially engineered steel bars that combine the processes of work hardening and heat treatment into a single, integrated procedure[1-5]. The quenching process used in the production of TMT Bars results in a high-strength, high-ductility material, even when made from inexpensive low-carbon steel[3-6]. These bars are typically manufactured using technologies such as Tempcore or Thermex, both of which utilize Quenching and Tempering (Q&T) methods to impart strength and desirable properties to the bars[2-7]. The process involves quenching the surface of

*Author for correspondence

the bar, followed by deformation and tempering, which results in a harder outer layer compared to the inner core[1-8].

To produce TMT Bars, industries use reheating furnaces that heat the bars to temperatures between 1200-1250°C, ensuring they are maintained at high temperatures before being rapidly water-cooled. The carbon content of the bars is carefully controlled to remain below 0.3%, which ensures good weldability without compromising the material's strength. Additionally, the carbon equivalent is maintained at or below 0.45%.

The key properties that make TMT Bars highly economical and safe for use are their strength, weldability, and ductility[1-8]. The TMT process enhances these properties, providing the bars with superior strength and corrosion resistance[8,9]. Controlled water cooling during production prevents the formation of coarse carbides, which are often responsible for the corrosive behaviour of steel bars[6-9]. TMT Bars also exhibit excellent workability and bendability, making them versatile for various construction applications[6-9].

TMT Bars are graded based on their yield strength, with common grades being Fe-415, Fe-500, Fe-550, and Fe-600[1-9]. They are available in diameters ranging from 8mm to 25mm, with standard lengths varying from 5 meters to 13 meters[1-9]. These bars are produced by both primary and secondary manufacturers, with integrated steel producers like TATA, SAIL, and JSW accounting for approximately 30% of the total rebar market[1-10]. The remaining market share is served by medium and small-scale producers, with around 300-400 secondary producers operating in the industry[1-10].

A new era in the Indian construction industry's economy has been ushered in with the introduction of TMT Bars. Since 1997 and 1998, when TMT Bars were widely used because of their ability to withstand corrosion, it has been a significant product[1-12]. They also demonstrated that RCC structures were more economical and had a longer lifespan[1-12]. TMT Bars are extensively utilized in high-rise buildings, bridges, flyovers, dams, general purpose concrete reinforcement constructions, and subterranean platforms for metros and transportation networks[1-12].

The manufacturing process begins with raw materials in furnaces, where the bar's chemical composition is controlled to achieve desired properties such as weldability, ductility, strength, and elongation during rolling[4-16]. After hot rolling, the steel bars pass through a specially designed water cooling chamber for quenching[5-16]. When the hot steel is immersed in water, a vapor blanket forms on the surface, slowing heat transfer[6-17]. Agitation removes this blanket, enhancing cooling[12-18]. Experimental parameters may include water pressure, rolling speed, finish rolling temperature, and cooling rate. The final heat treatment ensures the desired microstructure and properties[10-20].

TMT bars are known for their unique microstructure, with a hard martensitic surface and a softer ferrite-pearlite core, providing a balance of strength and ductility[1-20]. Quenching transforms the surface into martensite while the core remains austenitic. When etched with 2% Nital solution, three distinct rings appear: an outer martensitic ring, a semi-tempered martensite-bainite ring, and an inner ferrite-pearlite core[1-21].

The objective of this study on TMT bars from various brands is to ensure that the mechanical properties of the materials align with the specifications outlined in IS Standards 1786:1985. The samples used for comparison are of Fe-500 grade. This project aims to compare the mechanical properties of two brands under controlled conditions by conducting various tests, including hardness tests, corrosion tests, tensile tests, and welding parameter evaluations. These tests will provide valuable insights, helping users make a more informed decision when selecting the best material for their needs. By considering all relevant parameters and factors for both samples, the material with superior properties will be identified.

The specific objectives of this study are:

-To conduct mechanical tests, such as hardness and tensile tests, to assess the strength and durability of the materials.

-To perform electrochemical tests, such as corrosion tests, under different environmental conditions to evaluate the materials' resistance to corrosion.

2.0 Materials and Methods

Two distinct steel brands, both in their original condition, were chosen for the experiment. These samples meet IS 1786: 1985's requirements[1-4] for the Fe-500 grade. In this case, the TMT bar made by TATA is designated as "Sample A," whereas the TMT bar made by SAIL is

designated as "Sample B." In addition to other physical, mechanical, and chemical investigations, both samples are being evaluated for morphological analysis "using LEICA Optical Microscopy, model no. DM-2700M."

3.0 Results and Discussions

3.1 Composition Analysis

Strict restrictions on the alloying element composition are imposed by the Fe-500 grade steel standards to guarantee the material'squality and functionality. Inparticular, TMT bars must have a carbon content of no more than 0.3% and a carbon equivalent of no more than 0.42%. Low alloying elements like nickel (Ni), copper (Cu), and chromium (Cr) should only be included in trace amounts (up to 0.1%). Furthermore, the nitrogen level shouldn't be higher than 120 parts per million. For additional reference, Table I lists the chemical makeup of the two chosen brands. Carbon equivalent is calculated as:

Carbon Equivalent (C.E.)= %C + %Mn/6 + (%Cr + %Mo + %V)/5 + (%Cu + %Ni)/15

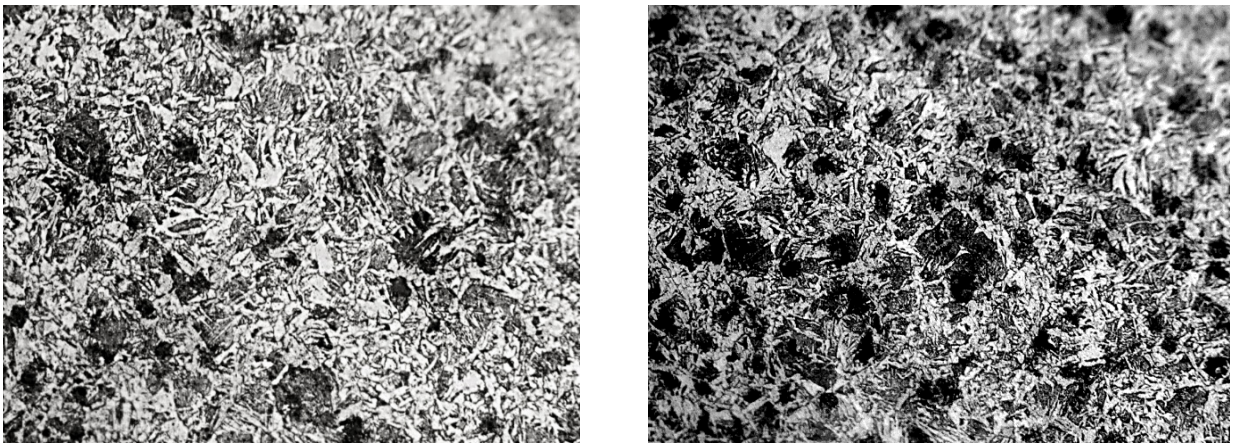
3.2 Microstructure

Brand TATA (Sample A) and Brand SAIL (Sample B) were both received in the same grade, Fe-500, and both samples had the same 16mm diameter. Following their polishing using emery sheets, these samples were sectioned transversely and their microstructures analyzed. A 2% Nital solution[16-21] was subsequently used to etch the samples in order to expose their microstructural characteristics. To capture the microstructures, optical micrographs were obtained as shown in Figure 1 to 2. Two micrographs were obtained of each sample, concentrating on the centre and the area close to the outer ring. To establish a baseline for comparison, these micrographs were taken under the same circumstances as they were received.

Upon comparing the microstructures of Samples A and B, it can be observed that the outer ring of

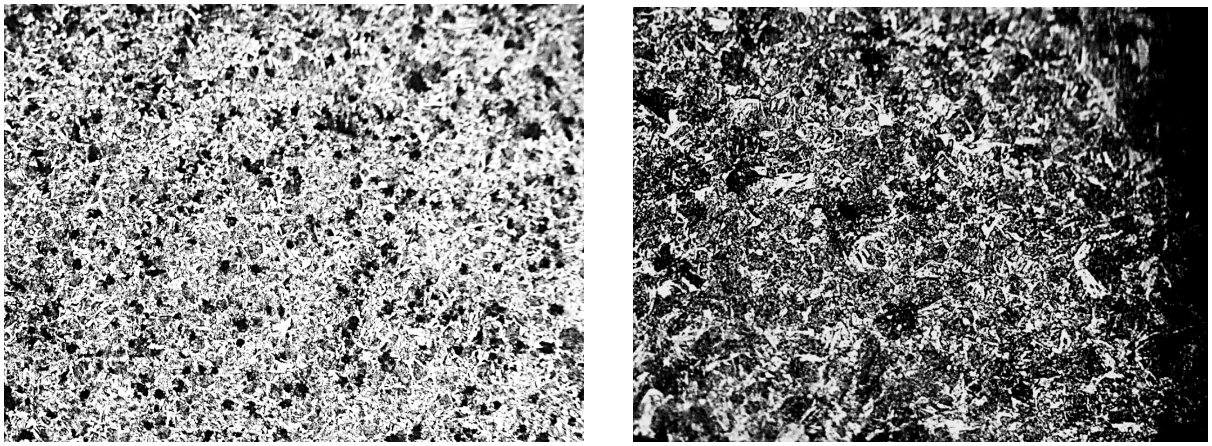
Table 1. Analysis of composition

Brand Name	% C	% Si	% S	% P	N	Micro-Alloying	C.E
Sample A	0.30 %	0.03%	0.055%	0.055%	120 ppm	0.2 %	0.42 %
Sample B	0.25 %	0.03%	0.050 %	0.050 %	100 ppm	0.3 %	0.39 %



(a) (b)

Figure 1. Optical micrograph for Sample A for **(a)** inner core and **(b)** outer ring at 200X magnification.



(a) (b)

Figure 2. Optical micrograph for Sample B for **(a)** inner core and **(b)** outer ring at 200X magnification.

both samples contains approximately 50% tempered martensite, while the inner core is composed of a ferritic-pearlitic structure. The tempered martensite present in the outer ring is characterized by a lath-like morphology, and the etched cross-section also reveals the presence of ferrite. The overall microstructure consists of four distinct phases: tempered martensite, bainite, pearlite, and ferrite. The volume fraction of martensite is primarily influenced by the carbon content in the material. The proportion of each phase present directly impacts the hardness of the samples, as different phases contribute varying degrees of resistance to deformation. Therefore, hardness testing is conducted after analyzing the micrographs to better understand the relationship between microstructure and mechanical properties.

3.3 Hardness

The hardness values were measured using a Vickers Hardness Tester (make by Fuel Instruments and Engineers Pvt Ltd, model no. VM 50) with a 20 kg load, taken at four distinct points along the cross-section of the same samples of Sample A and Sample B, spaced equally apart. It was observed that the hardness was higher near the outer edges of the samples compared to the centre or core region. This variation in hardness was found to correlate with the microstructure of the material, as the outer rim consisted primarily of martensite, while the inner region was predominantly composed of ferrite and pearlite. Martensite is a metastable phase of iron, enriched with carbon, which forms as a result of the diffusionless transformation of austenite during cooling. The increased hardness in the outer rim can be attributed to the severe lattice distortion caused by the formation of martensite. Therefore, the thicker the martensite rim, the harder the TMT bar, as the hardness is directly influenced by the extent of martensitic transformation at the surface. Hardness profile is shown in Figure 3.

The outer ring of the TMT bar samples exhibits a hardness range of Vickers Hardness Number (VHN) 260-290. This hardness is primarily influenced by the amount of martensite present in the outer ring, which

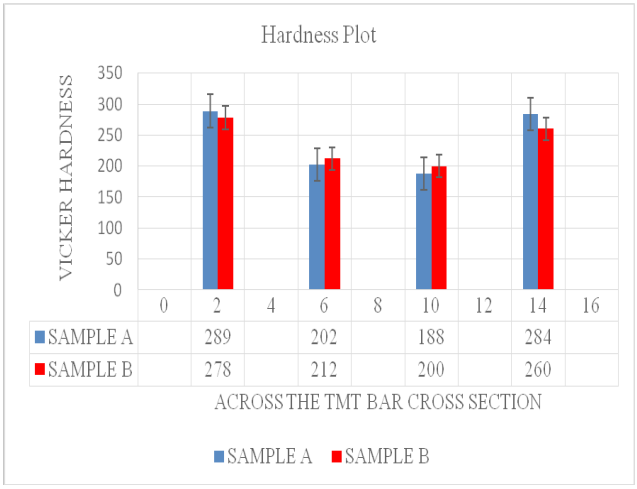


Figure 3. Hardness comparison of TMT Bars from different brands.

contributes to its increased hardness. In contrast, the inner core displays a lower hardness value, ranging from VHN 190-210, due to the presence of softer ferrite and pearlite phases. Based on these hardness values, it can be concluded that Sample A is harder at the outer surface compared to Sample B. Since hardness is closely related to tensile strength, this implies that Sample A likely possesses higher tensile strength than Sample B, as harder materials generally exhibit greater resistance to deformation and fracture under tensile loading.

3.4 Tensile Test

Tensile tests were conducted on both samples at a strain rate of 0.001/sec. The key material properties determined from these tensile tests included Young's modulus, yield stress, ultimate tensile stress, percentage elongation up to fracture, percentage reduction in cross-sectional area at fracture, and fracture stress. These properties are essential for understanding the material's mechanical behaviour under tensile loading. To ensure accurate and consistent results, both samples were prepared according to a standardized tensile test specimen design, which was specifically tailored for this type of testing. This design ensured that the samples were subjected to uniform stress and strain conditions, providing reliable data for further analysis.

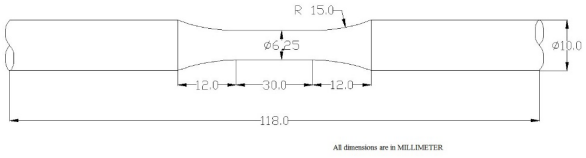


Figure 4. Tensile test specimen design.

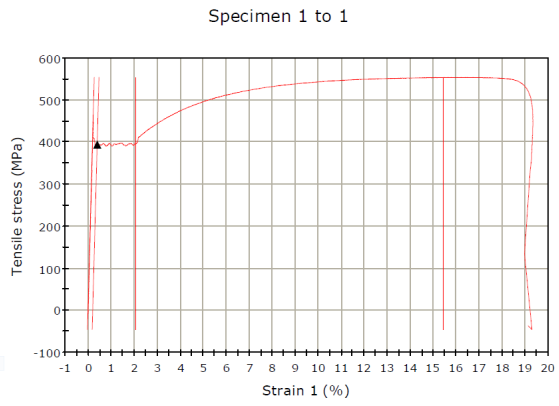


Figure 5. Stress-strain curve for sample A.

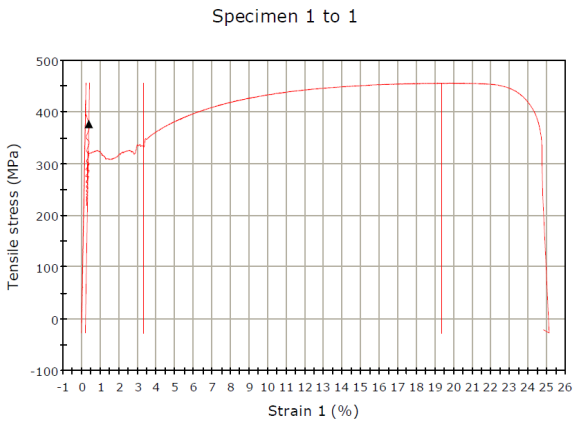


Figure 6. Stress-Strain Curve for sample B.

Table 2. Properties of TMT bars from different brands

Properties	Sample A	Sample B
Tensile Stress at Yield	394.444 MPa	376.870 MPa
Ultimate Tensile Stress	553.133 MPa	455.691 MPa
UTS/YS Ratio	1.40	1.21
Uniform Elongation	15.100%	19.915%
Reduction Area	72.211%	67.47%
Strain at Fracture	19.280%	24.732%
Strain Hardening Exponent	0.21593	0.24604

The tensile test yielded the stress-strain curve, which is displayed in Figure 5 and 6. The comparative analysis of the tensile test results and associated plots provides valuable insights into various factors that influence material properties. These factors are crucial for understanding the behaviour of materials under stress and play a significant role in determining their suitability for different applications. By examining these

properties, we can assess how materials perform under specific conditions, enabling the selection of the most appropriate materials for a wide range of engineering and industrial applications. Various properties are noted in Table 2.

3.5 Corrosion

Electrochemical tests were conducted on two different brands of materials, specifically focusing on the outer martensite rings. The key parameters measured during the investigation included corrosion potential (E_{corr}) and corrosion current (I_{corr}). Tafel extrapolation was employed as an efficient method for gathering corrosion data, making it particularly useful for small-sized specimens due to its simplicity and effectiveness. The Tafel extrapolation method involves plotting the logarithmic values of the current generated during an electrochemical reaction of the conducting metal in a solution, against the applied voltage, which is controlled by an electrical potential scanning device. This method utilizes data obtained from both cathodic and anodic polarization measurements. These polarization tests were carried out using a computer-controlled potentiostat, with a scan rate set at 1 mV/sec to ensure precise and accurate readings.

The results of the corrosion polarization studies, referenced against a standard calomel electrode, are presented in Table 3. The corrosion potential (E_{corr}) and corrosion current (I_{corr}) values listed in the table were experimentally derived from the cathodic and anodic polarization curves (voltage (E) vs. log current (I)). These values were obtained using the Tafel extrapolation method, which allows for the accurate calculation of

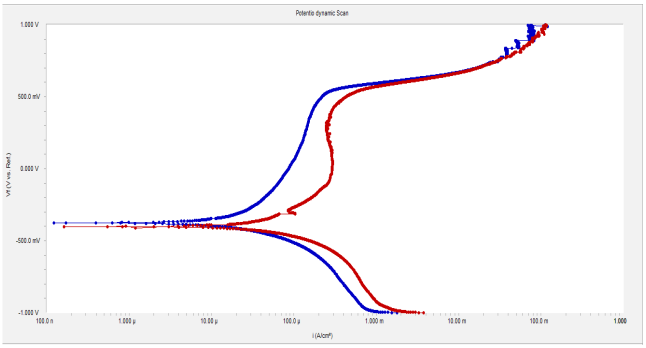


Figure 7. Potentio dynamic corrosion study of TMT bars from different brands (Blue for Sample A and red for Sample B).

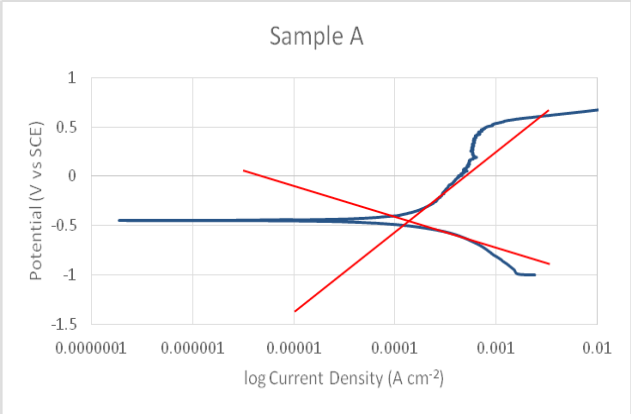


Figure 8. Potential (V) vs log Current Density (A/ cm^2) curve for Sample A.

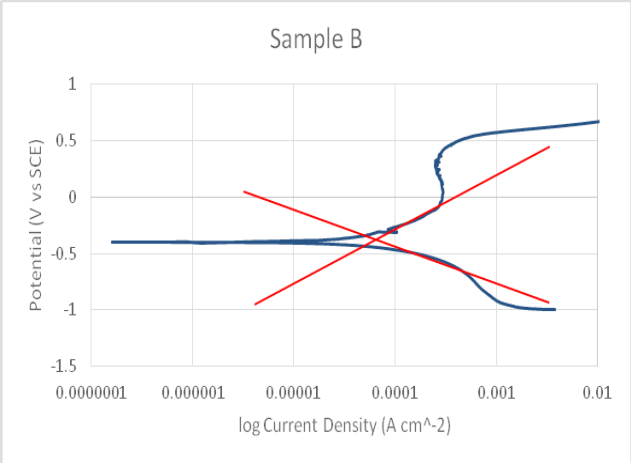


Figure 9. Potential (V) vs log Current Density (A/ cm^2) curve for Sample B.

corrosion parameters by analyzing the linear portions of the polarization curves.

A higher E_{corr}(corrosion potential) and I_{corr}(corrosioncurrent) value are indicative of a faster corrosion rate. In this case, Sample B exhibits higher E_{corr} and I_{corr} values compared to Sample A, suggesting that Sample B is less resistant to corrosion. As a result, the lifespan of Sample B is expected to be shorter than that of Sample A, since the faster corrosion rate will lead to quicker material degradation over time.

The duration of stagnant voltage at a specific current is directly related to the size of the passivity region; a longer stagnant voltage allows for the formation of a more extensive passivity region. In this case, Sample

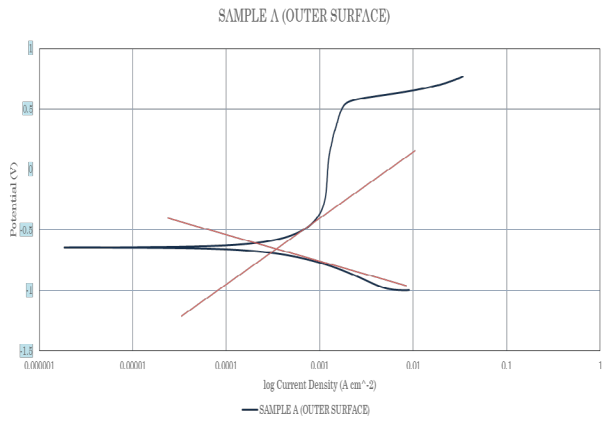


Figure 10. Potential (V) vs log Current Density (A/cm^2) curve for tensile treated Sample A.

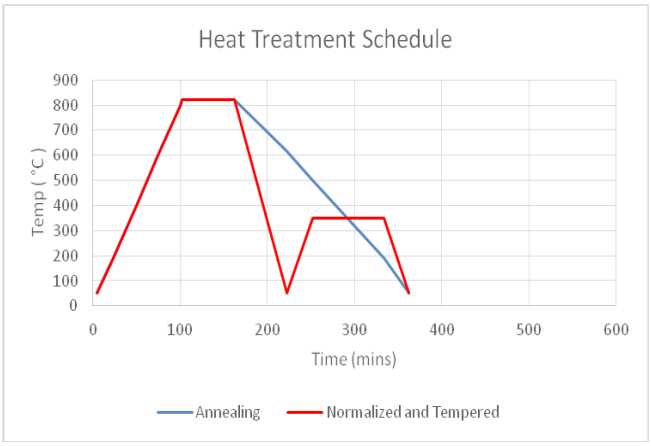


Figure 11. Heat Treatment Schedule for TMT bars of different brands.

B demonstrates a larger passivity region compared to Sample A, indicating that Sample B is more resistant to localized corrosion. This enhanced passivity behaviour suggests that Sample B has superior protective properties, making it more durable in corrosive environments.

Table 3. Corrosion properties of TMT bars from different brands

	E_{corr} (in Volt)	I_{corr} (in µA/cm^2)
Sample A	-0.447	150.02
Sample B	-0.402	79.81

Table 4. Corrosion properties for tensile treated TMTbars from different brands

	E_{corr} (in Volt)	I_{corr} (in µA/cm^2)
Tensile treated Sample A	-0.6 V	274
Tensile treated Sample B	-0.766 V	241

3.6 Heat Treatment

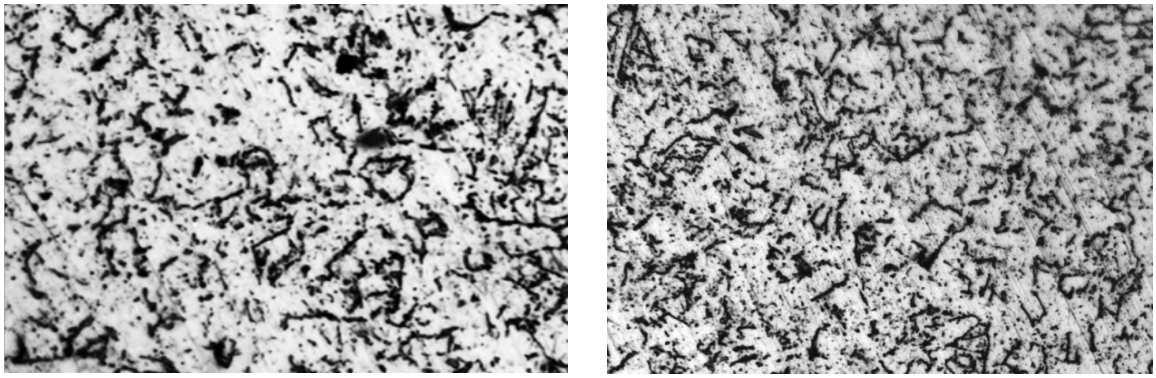
The as-received sample was in the form of a 16 mm diameter hot-rolled bar, featuring a core structure composed of ferrite and pearlite, with anouter ring of tempered martensite. The critical temperatures of the steel were determined based on its chemical composition, and the heat-treated specimen underwent a detailed microscopic examination to assess the resulting microstructure. The specimen was first heated to approximately 820°C to promote carbon enrichment in the austenite phase, followed by quenching to rapidly cool the material and then tempering to adjust the hardness and enhance the mechanical properties.

Small specimens were cut out for heat treatment, which was followed by corrosion behaviour analysis, hardness testing, and microscopic inspection. The following tests were performed on the samples of both brands:-

After 60 minutes at 820° C, let the furnace cool. - Hold at 820° C for 60 minutes, then let it cool naturally for another 60 minutes before tempering it at 350°C.

The microstructure of the specimen was examined using a light microscope after undergoing a meticulous preparation process. This involved metallographic polishing to achieve a smooth surface, followed by etching with a 2% nital solution. The etching process enhanced the visibility of the microstructural features, allowing for detailed observation and analysis under the microscope.

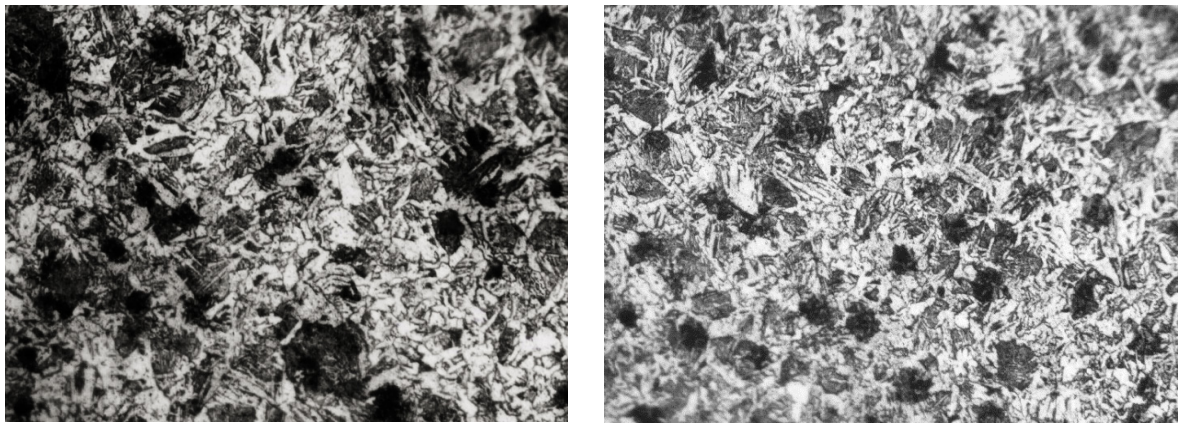
3.7 Annealed Microstructure



(a) (b)

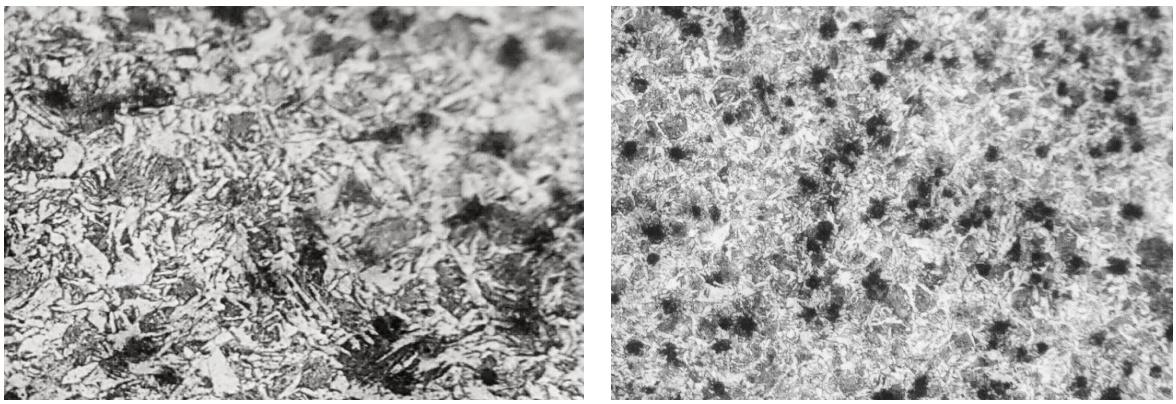
Figure 12. Annealed Microstructure of **(a)** Sample A and **(b)** Sample B at 200X magnification.

3.8 Normalized and Tempered Microstructure



(a) (b)

Figure 13. Normalized and Tempered Microstructure of **(a)** Sample A and **(b)** Sample B.



(a) (b)

Figure 14. Normalized and Tempered Microstructure of **(a)** Sample A and **(b)** Sample B at 200X magnification.

3.9 Corrosion Results after Heat Treatment

The corrosion test was conducted using a 0.9 M NaOH standard solution, also referred to as a pore solution. This basic solution was chosen because it closely simulates the typical environment where TMT bars are used, such as in concrete structures. Concrete generally maintains a pH range of approximately 8–9, making this solution an ideal medium for testing. Furthermore, it was observed that after heat treatment, the corrosion rate of the material significantly decreased, indicating an enhancement in its corrosion resistance due to the heat treatment process.

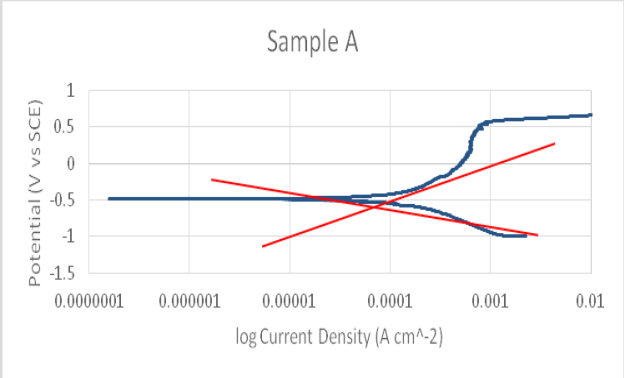


Figure 15. Potential (V) vs log Current Density (A/cm^2) curve for heat treated Sample A.

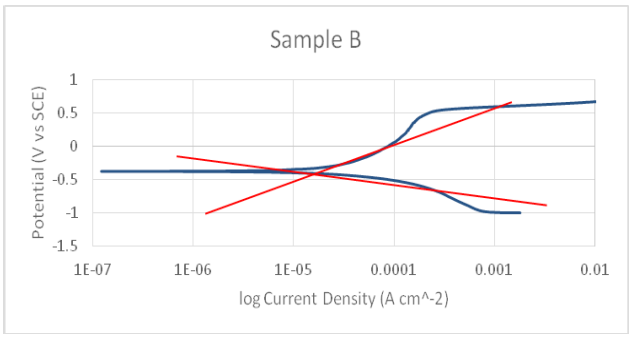


Figure 16. Potential (V) vs log Current Density (A/cm^2) curve for heat treated Sample B.

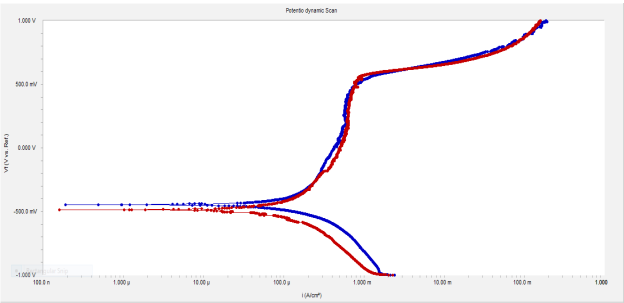


Figure 17. Potentio dynamic corrosion study of heat treated TMT bars from different brands (Blue for Sample A and red for Sample B).

Table 5. Corrosion properties for heat treated tmt bars from different brands

	E_{corr} (in Volt)	I_{corr} (in µA/cm^2)
Heat treated sample A	-0.503	74.57
Heat treated sample B	-0.408	16.87

4.0 Discussions

One of the significant accomplishments in the construction sector is the expanding market for TMT bars. As a result, even a minor variation in their properties could lead to customers opting for alternative manufacturers that offer products with superior or more desirable characteristics. Upon comparing the two samples, it was observed that the martensite content in the outer ring constituted approximately 50%. Meanwhile, the inner core consisted of a balanced distribution of ferrite and pearlite, with both phases present in nearly equal proportions.

-The hardness of Sample A was determined to be greater than that of Sample B in the outer regions. However, in the core region, Sample B exhibited higher hardness compared to Sample A. Since tensile strength is closely correlated with the hardness of a material, it can be inferred that Sample A possesses higher overall strength compared to Sample B.

-The I_{corr} value is directly proportional to the rate of corrosion, meaning that a higher I_{corr} value indicates a faster corrosion rate. Based on this principle, Sample B is observed to be more corrosion-resistant than Sample A. Consequently, the lifespan of Sample B is expected to be longer than that of Sample A. This conclusion can be attributed to the relationship between corrosion behavior and the martensite content in the material,

which plays a significant role in determining its corrosion resistance.

-The duration of stagnant voltage at a specific current is directly related to the extent of the passivity region; a longer stagnant voltage indicates a more extensive passivity region. In this context, Sample B exhibits a significantly larger passivity region compared to Sample A, suggesting that Sample B has superior passive behaviour and greater resistance to localized corrosion processes.

-The tensile test results indicate that Sample B is more ductile than Sample A, as evidenced by its greater uniform elongation. Furthermore, the stress-strain curve reveals that Sample A possesses higher yield strength and ultimate tensile strength compared to Sample B. This suggests that while Sample A excels in strength characteristics, Sample B demonstrates superior ductility, making it more suitable for applications requiring greater deformation without failure.

-The corrosion test conducted after tensile deformation indicates a reduction in corrosion resistance. This decrease can be attributed to the formation of a galvanic cell, which arises from the dislocations introduced during deformation. These dislocations create localized differences in electrochemical potential, promoting galvanic interactions that accelerate the corrosion process.

-The heat-treated material exhibits a noticeable reduction in corrosion rates, aligning with the predictions made earlier. This improvement in corrosion resistance can be attributed to the microstructural changes induced by the heat treatment process, which enhance the material's ability to withstand corrosive environments.

5.0 Conclusion

Sample A demonstrated superior strength characteristics, while Sample B exhibited greater ductility. In terms of corrosion resistance, Sample B outperformed Sample A, showcasing superior properties. Consequently, based on the overall evaluation, Sample B is the recommended choice over Sample A for constructing electric furnace or other equipment.

6.0 References

1. Allen DE. Statistical study of the mechanical properties of reinforcing bars [technical report]. Ottawa: Division of Building Research, National Research Council of Canada; 1972.
2. Perenchio WF. Corrosion of reinforcing steel. ASTM STP 169C; 1994. p. 164-72. https://doi.org/10.1520/STP36416S.
3. Berke NS. Corrosion inhibitors in concrete. Concrete International. 1991;13(7):24-7.
4. ASTM Standards. E7 Terminologies relating to metallography. E340 Test method for macro etching metals and alloys.
5. Barbara M, Walter S, Renzo V. Dual-phase steel rebars for high-ductile R.C. structures, Part 1: Microstructural and mechanical characterization of steel rebars. Eng Struct. 2007;29:3325-32. https://doi.org/10.1016/j.engstruct.2007.09.002.
6. Bimal KP, Surendera KJ. Impact toughness of high strength low alloy TMT reinforcement ribbed bar. Bull Mater Sci. 2002; 25(4):319-24. https://doi.org/10.1007/BF02704125.
7. Ray A, Mukerjee D, Sen SK, Batacharya A, Dhua SK, Prasad MS, Banerjee N, Popli AM, Sahu AK. Microstructure and properties of thermomechanically strengthened reinforcement bars: A comparative assessment of plain-carbon and low alloy steel grades. J Mater Eng Perform. 1997; 6(3):335-43. https://doi.org/10.1007/s11665-997-0098-9.
8. Dotreppe JC. Mechanical properties of quenched and self-tempered reinforcing steel at elevated temperatures compared with recommendations of Eurocode 2-Part1-2. Mater Struct. 1997; 30:430-8. https://doi.org/10.1007/BF02498567.
9. Kopeliovich D. Effect of alloying elements on the mechanical properties of steels [Internet]; 2009. Available from: https://biblio.univ-annaba.dz/ingeniorat/wp-content/uploads/2021/03/PFE-LAHMER-2020.pdf.
10. Ray A, Mukerjee S, Sen A, Bhattacharya G. Microstructure and properties of thermo-mechanically strengthened reinforcement bars: A comparative assessment of plain-carbon and low-alloy steel grades. J Mater Eng Perform. 1997. https://doi.org/10.1007/s11665-997-0098-9.
11. Mukhopadhyay A, Galasso L. Better control for mechanical properties of quenched and tempered bars. Tecnol Metal Mater Miner. São Paulo. 2011.
12. Keleştemur O, Yıldız S. Effect of various dual-phase heat treatments on the corrosion behavior of reinforcing steel used in reinforced concrete structures. Constr Build Mater. 2009; 23(1):78-84. https://doi.org/10.1016/j.conbuildmat.2008.02.001.

13. Broomfield JP. Corrosion and residual life in concrete structures-an overview. Bull Electrochem. 1995; 11(3):121.
14. Neethu N, Rajan N, Sandeep S. A study on variation of hardness of TMT and normalised steel bars under cold work [technical report]. 2017. https://doi.org/10.13140/RG.2.2.24423.21927.
15. Das S. Failure analysis of re-bars during bending operations. Case Stud Eng Fail Anal. 2014; 2(2):51-3. https://doi.org/10.1016/j.csefa.2014.04.003.
16. Islam MA. Corrosion behaviours of high strength TMT steel bars for reinforcing cement concrete structures. Procedia Eng. 2015; 125:623-30. https://doi.org/10.1016/j.proeng.2015.11.084.
17. Rifai M, Miyamoto H, Fujiwara H. Effects of strain energy and grain size on corrosion resistance of ultrafine grained Fe-20%Cr steels with extremely low C and N. Int J Corros. 2015; 2015:1-9. https://doi.org/10.1155/2015/386865.
18. Kumar P. Study report on failure analysis of TMT bar due to steel defects. Int J Sci Res Eng Trends. 2020; 6(6):3710-2.
19. Prasad A, Kumar N, Saini R, Singh S, Kanjilal P. Complete quality control of TMT steel bar and high strength structural steel plates sections and prestressed concrete for total integrity of the final structure. Mater Today Proc. 2022; 67(4):543-9. https://doi.org/10.1016/j.matpr.2022.07.359.
20. Pathak H, Lodha Y, Mahajan YY. A case study of bending of TMT steel bars. Int J Eng Res Technol. 2015; 4(5):285-8. https://doi.org/10.17577/IJERTV4IS050454.
21. Majhi M. Experimental analysis of water pressure quenching rate on TMT bar and physical properties. Int Res J Mod Eng Technol Sci. 2022; 4(6):285-91.